

IEICE **TRANSACTIONS**

on Electronics

DOI:10.1587/transele.2024RES0003

Publicized:2024/09/06

**This advance publication article will be replaced by
the finalized version after proofreading.**

A PUBLICATION OF THE ELECTRONICS SOCIETY



The Institute of Electronics, Information and Communication Engineers

Kikai-Shinko-Kaikan Bldg., 5-8, Shibakoen 3chome, Minato-ku, TOKYO, 105-0011 JAPAN

BRIEF PAPER

Optimized mode coefficients of multimode horn with square aperture achieving constant beamwidths for multiband use

Hiroyuki DEGUCHI^{†a)}, Senior Member, Masataka OHIRA^{†b)}, and Mikio TSUJI^{†c)}, Members

SUMMARY This paper proposes directivity synthesis for multimode horns with square-waveguide aperture based on quadratic programming approach using radiation patterns for each mode for obtaining axial-symmetric beam and low cross-polarization components, and also for realizing desired constant beamwidth. As a design example, we present a 11/14/20/30-GHz primary horn with square aperture and also show effectiveness of the proposed method by evaluating electric force lines of aperture distribution and 15-dB beamwidth of radiation patterns.

key words: Horn antennas, quadratic programming, low cross-polarization, rectangular waveguide, optimization.

1. Introduction

The radiation characteristics of a horn antenna can be calculated from the aperture-field method[1] using the electromagnetic fields on the antenna aperture, which are determined by the mode coefficients of the horn waveguide[2]. This means we can know the aperture fields or the mode coefficients required to get a desirable radiation characteristic. In conventional multimode horns, higher-order modes are controlled to reduce cross-polarization components[3]–[6], and also to enhance the co-polarization component[7] by directivity synthesis based on the quadratic programming approach[8]. This technique has been applied to Cassegrain antennas[9] and circular aperture multimode horns[10], [11]. However, none of these design methods consider multiple frequency bands, such as multiband antennas. For example, in order to use such an antenna as a primary horn of multiband reflector antenna, it is necessary to maintain a constant beamwidth independent of the frequency. When frequency bands are close, as in the 12/14 GHz band[12], the design is relatively straightforward. In the case of multiple separate bands such as 20/30/44 GHz[13] and Ku/Ka bands[14], although cross-polarization components have been reduced, the beamwidth becomes narrower as the frequency increases. So it is an extremely challenging design to maintain a constant beamwidth over multiple frequency bands.

This paper proposes a novel directivity synthesis approach for the design of multimode horn that not only achieves axial-symmetric and low cross-polarization characteristics, but also controls the main beam shape over a wide frequency range. For the first time, we clarify the mode coefficients maintaining a constant beamwidth and gain. As

[†]The authors are with the Faculty of Science and Engineering, Doshisha University, Kyotanabe-shi, 610-0321 Japan.

a) E-mail: hdeguchi@mail.doshisha.ac.jp

b) E-mail: mohira@mail.doshisha.ac.jp

c) E-mail: mtsuji@mail.doshisha.ac.jp

a design example, mode coefficients of a multimode horn with a square aperture in the 11/14/20/30 GHz bands, which are commonly used frequencies for satellite communication and broadcasting, is optimized. The effectiveness of the proposed approach is confirmed from the electric field vector on the aperture and the co- and cross-polarization components of radiation patterns.

2. Design procedure

Figure 1 shows a waveguide horn antenna with a square aperture of $a \times a$. The coordinate origin is at the center of the aperture, where (\bar{x}, \bar{y}) represents normalized Cartesian coordinates, and the observation point P is represented in spherical coordinates (r, θ, ϕ) . The radiation pattern based on the mode functions given in Appendix A can be calculated by using the aperture-field method.

The gain of the horn antenna is optimized under the evaluation function expressed as a quadratic equation in terms of unknown mode coefficients. If the constraints are linear, the quadratic programming approach can be applied to the design of the multimode horn. For a square-aperture multimode horn, when the directivity in the boresight direction ($\theta = 0$) is set as a constant in the form of an equality constraint, the gain G can be written as follows:

$$G|_{\theta=0} = \frac{4\pi}{P_t}, \quad P_t = \sum_{j=1}^N C_j^2. \quad (1)$$

Thus, the directivity synthesis becomes a problem of minimizing the quadratic equation P_t about the mode coefficients C_j .

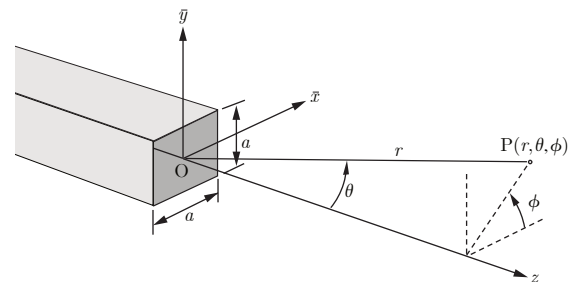


Fig. 1 Coordinate systems for waveguide horn with square aperture.

(1) Axial symmetric and low cross-polarization characteristics

To obtain an axial symmetric main beam, the inequality constraint for $\phi_1 = 0^\circ$, $\phi_2 = 90^\circ$, and $\phi_0 = 45^\circ$, which limits the amplitude of the deviation from the axial symmetric main beam to $B (> 0)$, leads to the following linear equation in terms of the unknown coefficients C_j .

$$\begin{aligned} -B &\leq F_{\text{co}} \Big|_{\phi_i} - F_{\text{co}} \Big|_{\phi_0} \quad (i = 1, 2) \\ &= \sum_j C_j \left\{ f_{\text{co},j}(\theta, \phi_i) - f_{\text{co},j}(\theta, \phi_0) \right\} \\ &\leq B \quad (0 \leq \theta \leq \theta^{(b)}) \end{aligned} \quad (2)$$

with

$$F_{\text{co}}(\theta, \phi) = \sum_j C_j f_{\text{co},j}(\theta, \phi), \quad (3)$$

where $F_{\text{co}}(\theta, \phi)$ is the co-polarization component of far-field radiated by multiple modes, $f_{\text{co},j}(\theta, \phi)$ is the co-polarization component of j th mode, and $\theta^{(b)}$ represents the angular range of the axial symmetric main beam to be achieved.

On the other hand, without incorporating the conditions of cross-polarization cancellation[15] of the universal radiation pattern as shown in Appendix B, we consider here inequality constraints to limit the peak amplitude of the cross-polarization level to $X (> 0)$ ($i = 0, 1, 2$).

$$-X \leq F_{\text{cr}} \Big|_{\phi_i} = \sum_j C_j f_{\text{cr},j}(\theta, \phi_i) \leq X \quad (0 \leq \theta \leq \theta^{(x)}) \quad (4)$$

with

$$F_{\text{cr}}(\theta, \phi) = \sum_j C_j f_{\text{cr},j}(\theta, \phi), \quad (5)$$

where $\theta^{(x)}$ represents the upper limit of the range of the cross-polarization region, and the cross-polarization component F_{cr} is also a linear equation in terms of the unknown coefficients C_j , and $f_{\text{cr},j}(\theta, \phi)$ is the cross-polarization component of j th mode. Similarly, it is possible to impose inequality constraints to reduce the peak sidelobe level to a certain value or below.

(2) Main beam shape

In this paper, to achieve the desired main beam shape, we further define inequality constraints for the beamwidth at $\theta = \theta_i^{(w)}$ to have an amplitude of $W_b \pm \Delta W$ ($W_b \gg \Delta W > 0$) as follows.

$$W_b - \Delta W \leq \sum_{j=1}^N C_j f_{\text{co},j}(\theta_i^{(w)}, \phi_i) \leq W_b + \Delta W, \quad (6)$$

where the angle $\theta_i^{(w)}$ represents the beamwidth at ϕ_i .

Instead of the above conditions, if we need the amplitude of the main beam to be at least $W(\theta)$ for the angular range $0 \leq \theta < \theta_i^{(w)} (< \theta_i^{(0)})$ for each $i = 0, 1, 2$, the constraint for the main beam shape is as follows:

$$W(\theta) \leq F_{\text{co}} \Big|_{\phi_i} = \sum_{j=1}^N C_j f_{\text{co},j}(\theta, \phi_i) \quad (0 \leq \theta < \theta_i^{(w)}) \quad (7)$$

We now consider a horn structure that is rotationally symmetric by 90° around the central axis. If the coefficients of TE/TM_{*mn*} modes (m and n : mode indices) are set to be equal to those of the orthogonal polarized TE/TM_{*nm*} modes, the same radiation pattern can be obtained for orthogonal polarizations.

3. 11/14/20/30 GHz band primary horn

Considering the multiband use of primary horns, we optimize mode coefficients using the directivity synthesis approach with the main beam shape control as shown in Sec. 2 (1) to maintain a constant beamwidth of $38.5^\circ \times 38.5^\circ$ independent of the frequency.

(1) 11/14 GHz band

As the first example, we optimize mode coefficients of the horn antenna with a constant beamwidth of $38.5^\circ \times 38.5^\circ$ in the 11/14 GHz band (11.7–12.2 GHz, 12.25–12.75 GHz, and 14.0–14.5 GHz). This optimization is achieved using the inequality constraint in Eq. (7) with $W_b = -15$ dB. To accomplish this goal, we consider the mode number $N = 6$, that is, TE₁₀, TE/TM₁₂, TE₃₀ modes, and TE/TM₃₂ modes. In order to eliminate the cross-polarization components, it is necessary to excite both TE_{*mn*} and TM_{*mn*} modes together, as shown in Appendix B. Figure 2 (a) illustrates stream plot of the electric field vector $\mathbf{E}_t = E_x \mathbf{a}_x + E_y \mathbf{a}_y$ (see Appendix C) on the aperture and contour plot of the co-polarization component $E_y^\eta(x, y) = E_y(x, y)/E_y(0, 0)$, where \mathbf{a}_x and \mathbf{a}_y are unit vectors of x and y directions, respectively. Also Fig. 2 (b) shows radiation pattern normalized by maximum gain at the central frequency 11.95 GHz in the 11 GHz band. The level in the direction $\theta = 0$ means aperture efficiency. The mode coefficients obtained by the proposed method are listed in the figure caption. In Fig. 2, the angles where the relative radiation power to the front reaches -15 dB are $\theta = 38.5^\circ$ for $\phi = 0^\circ, 90^\circ$ (shown as dashed lines in the figure), and $\theta = 39.1^\circ$ for $\phi = 45^\circ$. The peak sidelobe level is -34.0 dB, the gain is 14.9 dBi, and the aperture efficiency is 76.7%. Similarly, at the central frequency 14.25 GHz in the 14 GHz band as shown in Fig. 3, the angles where the relative radiation power reaches -15 dB are $\theta = 38.5^\circ$ for all $\phi = 0^\circ, 45^\circ, 90^\circ$ (indicated by dashed lines in the figure). The peak sidelobe level is -32.5 dB, indicating that a constant predetermined beamwidth is achieved. In this case, although the aperture efficiency decreases to 64.5%, the gain at 14.25 GHz remains almost the same as that at 11.95 GHz.

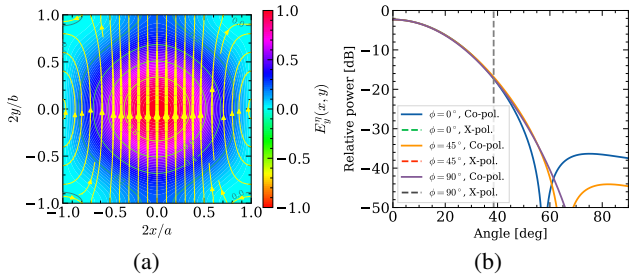


Fig. 2 (a) The electric field vector of the aperture and (b) radiation pattern as a function of angle θ at 11.95 GHz optimized with mode number $N = 6$ in a square aperture $51 \times 51 \text{ mm}^2$, where the peak level is normalized by maximum gain. The mode coefficients of TE_{10} , TE/TM_{12} , TE_{30} , and TE/TM_{32} are 0.879, -0.212 , 0.420, -0.079 , -0.005 , and -0.008 , respectively.

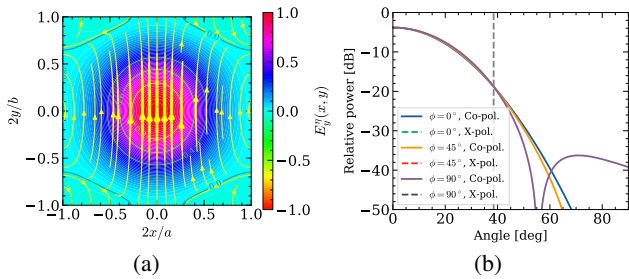


Fig. 3 (a) The electric field vector of the aperture and (b) radiation pattern as a function of angle θ at 14.25 GHz optimized with mode number $N = 6$ in a square aperture $51 \times 51 \text{ mm}^2$, where the peak level is normalized by maximum gain. The mode coefficients of TE_{10} , TE/TM_{12} , TE_{30} , and TE/TM_{32} are 0.780, -0.265 , 0.526, -0.188 , 0.082, and -0.057 , respectively.

(2) 20 GHz band

To add the 20 GHz band (17.7–21.2 GHz) to 11/14 GHz band, we consider the mode number $N = 13$, which includes TE_{10} , TE/TM_{12} , TE_{30} , TE/TM_{32} , TE/TM_{14} , TE/TM_{34} , TE_{50} , TE/TM_{52} modes, and further optimize their mode coefficients by adding the inequality constraint equation of $W(\theta) = \cos^n \theta$ as in Eq. (7). The results are shown in Fig. 4. From the figure, it can be confirmed that the same beamwidth (with constant gain) as in the 11/14 GHz band is achieved at 19.45 GHz. However, the aperture efficiency is reduced to 47.3%.

(3) 30 GHz band

To add the 30 GHz band (27.5–31.0 GHz) to 11/14/20 GHz band, further optimization is performed considering the mode number $N = 20$, that is, TE_{10} , TE/TM_{12} , TE_{30} , TE/TM_{32} , TE/TM_{14} , TE/TM_{34} , TE_{50} , TE/TM_{52} , TE/TM_{16} , TE/TM_{54} , TE/TM_{36} , TE_{70} modes. Figure 5 illustrates the electric field vector on the aperture and radiation pattern at 27.5 GHz, where the angles corresponding to a relative radiation power of -15 dB are $\theta = 38.5^\circ$ for $\phi = 0^\circ$ and 90° , $\theta = 39.4^\circ$ for $\phi = 45^\circ$ (dashed lines in the figure). The peak sidelobe level is -37.2 dB . The gain is 15.1 dBi, and the aperture efficiency is 32.3%. Comparing the relative patterns to the peak value in Figs. 2–5 (b), it can be confirmed

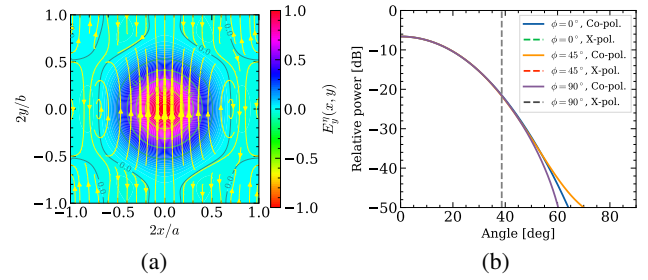


Fig. 4 (a) The electric field vector of the aperture and (b) radiation pattern as a function of angle θ at 19.45 GHz optimized with mode number $N = 13$ in a square aperture $51 \times 51 \text{ mm}^2$, where the peak level is normalized by maximum gain. The mode coefficients of TE_{10} , TE/TM_{12} , TE_{30} , TE/TM_{32} , TE/TM_{14} , TE/TM_{34} , TE_{50} , and TE/TM_{52} are 0.619, -0.283 , 0.565, -0.309 , 0.236, -0.157 , 0.045, -0.181 , -0.040 , 0.056, 0.045, -0.008 , and 0.003, respectively.

that a constant beamwidth has been achieved.

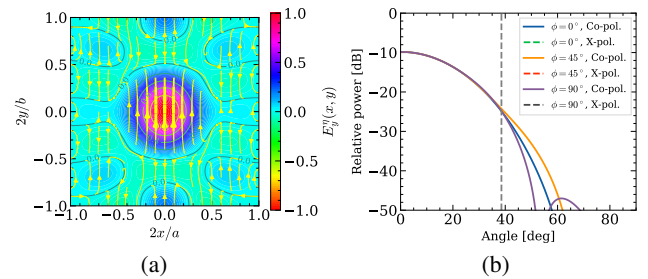


Fig. 5 (a) The electric field vector of the aperture and (b) radiation pattern as a function of angle θ at 27.5 GHz optimized with mode number $N = 20$ in a square aperture $51 \times 51 \text{ mm}^2$, where the peak level is normalized by maximum gain. The mode coefficients of TE_{10} , TE/TM_{12} , TE_{30} , TE/TM_{32} , TE/TM_{14} , TE/TM_{34} , TE_{50} , TE/TM_{52} , TE/TM_{16} , TE/TM_{54} , TE/TM_{36} , and TE_{70} are 0.441, -0.246 , 0.492, -0.334 , 0.306, -0.204 , 0.085, -0.339 , -0.151 , 0.203, 0.176, -0.075 , 0.030, -0.014 , 0.078, 0.083, -0.066 , -0.051 , 0.102, and -0.049 , respectively.

(4) Frequency characteristics

Figure 6 summarizes the frequency characteristics of the 15-dB beamwidth for the cases with mode numbers $N = 6, 8, 13$, and 20, comparing with a conventional result for the mode number $N = 4$ without main beam control. It clearly demonstrates that the beamwidth can be kept constant over a wide frequency range by using the proposed mode coefficients. The frequency characteristics of the aperture efficiency are shown in Fig. 7. In the case of the directivity synthesis without main beam control ($N = 4$), the aperture efficiency remains constant. However, when maintaining a constant beamwidth, the aperture efficiency decreases as the frequency increases. This is expected from the fact that the aperture field distribution normalized by each wavelength becomes almost constant.

4. Conclusion

The proposed optimization method aims to synthesize the directivity of a square waveguide horn antenna, achieving

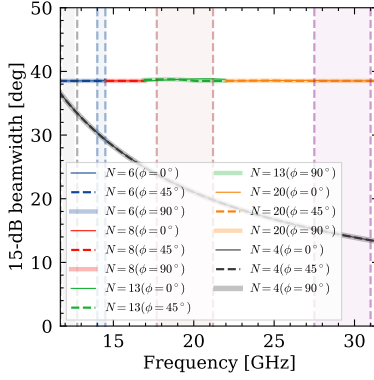


Fig. 6 Comparison of frequency characteristics of 15-dB beamwidth.

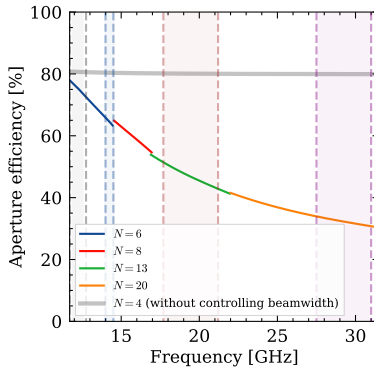


Fig. 7 Comparison of the frequency characteristics of the aperture efficiency. In the case of $N = 4$, there is no main beam control, while for $N = 6, 8, 13, 20$, main beam control is implemented.

axial symmetric and low cross-polarization characteristics while realizing the desired main beam shape. Through the design examples, we presented the optimal mode coefficients for a primary horn used in the 11/14/20/30 GHz bands, and demonstrated the ability to maintain a constant 15-dB beamwidth over all frequencies.

Acknowledgement

This work was supported in part by the Grant-in-Aid for Scientific Research (C) (20K04475) from Japan Society for the Promotion of Science(JSPS).

References

- [1] R. F. Harrington, *Time-Harmonic Electromagnetic Fields*, Wiley-IEEE Press, New York (2001).
- [2] S. Silver, *Microwave Antenna Theory and Design*, McGraw-Hill, New York (1949).
- [3] T. Kitsuregawa, *Advanced Technology in Satellite Communication Antennas*, 1.3.1 Dual-mode conical horns, pp. 71–73, Artech House, London (1990).
- [4] H. Deguchi, M. Tsuji and H. Shigesawa, “Compact low-cross-polarization horn antennas with serpentine-shaped taper,” *IEEE Trans. Antennas Propagat.*, **52**[10], pp. 2510–2516 (2004).
- [5] T. Kobayashi, H. Deguchi, M. Tsuji and K. Omori, “Compact multimode horn with coaxial corrugation for circular coverage,” *IEICE*

Trans. Commun., **E93-3**[1], pp. 32–38 (2010).

- [6] R. Omi, R. Wakabayashi, H. Deguchi and M. Tsuji, “Multimode horn antennas with square aperture loading grooves for circular beam and low cross-polarization characteristic,” *Proceedings of International Symposium on Antennas and Propagation 1*, pp. 489–490 (2018).
- [7] N. Goto, F. Watanabe and T. Sekiguchi, “The optimum directivity of array antennas with a specified sidelobe level,” *Trans. IECE, Japan*, **E60**[8], pp. 399–402 (1977).
- [8] “IMSL Math/Library Volumes 1 and 2, Chapter 8,” Visual Numerics, Inc., p. 982 (1997).
- [9] N. Goto and F. Watanabe, “The optimum aperture efficiency of Cassegrain antennas with a specified sidelobe level,” *IECE Trans. B*, **J61**[5], pp. 321–326 (1978).
- [10] H. Deguchi and M. Tsuji, “Radiation-pattern synthesis based on quadratic programming for multimode circular horns,” *Proceedings of 2006 Progress In Electromagnetics Research Symposium*, 1, p. 435 (2006).
- [11] H. Deguchi, M. Tsuji and H. Watanabe, “Low-sidelobe multimode horn design for circular coverage based on quadratic programming approach,” *IEICE Trans. Commun.*, **E-91-C**[1], pp. 3–8 (2008).
- [12] H. Deguchi, T. Goto, M. Tsuji, H. Shigesawa and S. Matsumoto, “Multimode horn with low cross polarization optimized for dual-band use,” *IEICE Trans. Commun.*, **E87-B**[9], pp. 2777–2782 (2004).
- [13] C. Granet and G. L. James, “Optimized Spline-Profile Smooth-Walled Tri-Band 20/30/44-GHz Horns,” *IEEE Trans. Antennas Wireless Propagation Letters.*, **6** pp. 492–494 (2007).
- [14] P. Zhang, J. Qi and J. Qiu, “Efficient design of a novel wide-illumination-angle Ku/Ka-band feed for reflector antennas,” *Proceedings of International Symposium on Antennas and Propagation 1*, pp. 814–815 (2016).
- [15] J. L. Volakis, *Antenna Engineering Handbook*, 4ed, Chapter 14, Horn antennas, p.14-24, McGraw-Hill, New York (2007).

Appendix A: Mode functions of electric field for square waveguide

The mode function $e_{[mn]}$ of the TE_{mn} mode in a square waveguide is given by

$$e_{[mn]} = A_{mn} \left[\frac{n\pi}{b} \cos \frac{m\pi}{2} (\bar{x} + 1) \sin \frac{n\pi}{2} (\bar{y} + 1) \mathbf{a}_x - \frac{m\pi}{a} \sin \frac{m\pi}{2} (\bar{x} + 1) \cos \frac{n\pi}{2} (\bar{y} + 1) \mathbf{a}_y \right], \quad (\text{A} \cdot 1)$$

where (\bar{x}, \bar{y}) represents the normalized coordinate system.

$$\bar{x} = \frac{2}{a}x, \quad \bar{y} = \frac{2}{b}y \quad (\text{A} \cdot 2)$$

Also, the mode function of the electric field for the TM_{mn} mode, denoted as $e_{(mn)}$, is given by

$$e_{(mn)} = -A_{mn} \left[\frac{m\pi}{a} \cos \frac{m\pi}{2} (\bar{x} + 1) \sin \frac{n\pi}{2} (\bar{y} + 1) \mathbf{a}_x + \frac{n\pi}{b} \sin \frac{m\pi}{2} (\bar{x} + 1) \cos \frac{n\pi}{2} (\bar{y} + 1) \mathbf{a}_y \right]. \quad (\text{A} \cdot 3)$$

The normalization coefficient of the mode, denoted as A_{mn} , is described as follows:

$$A_{mn} = \frac{1}{\pi} \sqrt{\frac{ab\epsilon_m\epsilon_n}{(mb)^2 + (na)^2}} \quad (\text{A} \cdot 4)$$

with

$$\epsilon_m = \begin{cases} 1 & (m = 0) \\ 2 & (m = 1, 2, \dots) \end{cases} \quad \epsilon_n = \begin{cases} 1 & (n = 0) \\ 2 & (n = 1, 2, \dots) \end{cases} \quad (\text{A}\cdot 5)$$

Appendix B: Cross-polarization elimination conditions for universal radiation patterns

When the aperture dimensions $a \times b$ are sufficiently large, the relationship between the coefficients $C_{[mn]}$ and $C_{(mn)}$ of the TE_{mn} and TM_{mn} modes, respectively, for eliminating the cross-polarization component of higher-order modes excited by the dominant TE_{10} mode, is as follows.

$$C_{(mn)} = \mp \frac{a}{b} \frac{n}{m} C_{[mn]} \quad (\text{A}\cdot 6)$$

The upper sign indicates the case where the electric field vectors of the cross-polarization components of both modes are in the same direction, while the lower sign indicates the opposite case. In case of excitation using orthogonal TE_{01} mode, the relationship between the coefficients $C'_{[nm]}$ and $C'_{(nm)}$ of the TE_{mn} and TM_{mn} modes, respectively, can be expressed as follows.

$$C'_{(nm)} = \mp \frac{b}{a} \frac{n}{m} C'_{[nm]} \quad (\text{A}\cdot 7)$$

Appendix C: Aperture field distribution due to multiple modes

The aperture electric field distribution \mathbf{E}_t due to multiple modes is expressed as

$$\mathbf{E}_t = \sum_{m,n} C_{[mn]} \sqrt{Z_{[mn]}} \mathbf{e}_{[mn]} + \sum_{m,n} C_{(mn)} \sqrt{Z_{(mn)}} \mathbf{e}_{(mn)} \quad (\text{A}\cdot 8)$$

with

$$Z_{[mn]} = \frac{\omega\mu}{\beta_{[mn]}}, \quad Z_{(mn)} = \frac{\beta_{(mn)}}{\omega\epsilon}, \quad (\text{A}\cdot 9)$$

where $Z_{[mn]}$ and $Z_{(mn)}$ are impedances, $\beta_{[mn]}$ and $\beta_{(mn)}$ indicates phase constants of TE_{mn} mode and TM_{mn} mode, respectively, and also ω is the angular frequency, ϵ is the permittivity, and μ is the permeability of the medium.